Optimization of multi-layer ceramic capacitor geometry for maximum yield during binder burnout

B. PETERS, S. J. LOMBARDO
Department of Chemical Engineering, University of Missouri, Columbia, MO 65211, USA
E-mail: Lombards@Missouri.edu

The yield during binder burnout of barium titanate multi-layer ceramic capacitors with poly(vinyl) butyral as a binder and platinum as the electrode material depends on the side length and height of the devices. In general, the yield decreases with increasing volume of the capacitor and depends on the aspect ratio of the component. For capacitors of square parallelepiped geometry, the optimum aspect ratio determined from the analysis of binder burnout yield data occurs at a height-to-length ratio of approximately 1 : 3. A methodology is presented which describes how to use the yield data obtained from binder burnout experiments to guide the optimum design of capacitor geometry. Analytical expressions were developed for capacitors of cube, square parallelepiped, rectangular parallelepiped, circular cylinder, and elliptical cylinder geometry. As the dependence of the yield on the dimensions becomes more complex, the optimum shape of the capacitor becomes more asymmetric.

1. Introduction

The fabrication of multilayer ceramic capacitors (MLCs) involves a sequence of a large number of processing operations, with production losses associated with each step. Of these, binder burnout [1] generally requires the longest time and often results in a significant amount of product rejection. Two other drawbacks related to binder burnout are that the development of the heating schedules is often a trial-and-error procedure, and a heating cycle developed for a particular capacitor geometry and size may not be satisfactory for components of different shape and dimensions.

From a theoretical viewpoint, failure of multilayer devices during the binder burnout process occurs when a local internal stress exceeds the local strength of the material. These stresses arise from capillary forces accompanying migration of liquid binder and hydrostatic forces associated with the generation of gas-phase decomposition products. Both types of stresses are not constant but vary temporally and spatially during the burnout cycle. As these stresses are changing, the local strength of the composite capacitor is also changing as binder is removed. Whereas the initial MLC green strength of order 1–10 MPa is sufficient for handling the green components, the reduction in green strength after the binder is removed is so drastic as to preclude handling of the bodies.

A number of failure modes are observed in MLCs that do not survive the burnout cycle. Blisters or bubbles arise when the generation of gas-phase products exceeds some critical pressure within the body. These two types of defects arise when the volume fraction of the binder is still sufficiently high as to constitute a continuous film. Failure under these conditions corresponds to the MLCs still having some elasticity from the binder phase.

Other types of defects that arise such as cracks, delamination, and complete fracture of the component correspond to a brittle mode of failure. For brittle fracture, Weibull [2–5] statistics are most often used to describe the probability of failure. With this formalism, which is based upon the theory of the weakest link, the number of flaws present increases as the volume is increased, or in other words, the probability of failure will increase as the sample size is increased. This was represented by Weibull [2] as the probability of failure, S, for an isotropic material as $S = 1 - \exp\left(-\int_V n(\sigma)\mathrm{d}V\right)$, where $n(\sigma)$ is a function expressing the strength properties of a material. From the form of S, it is clear that as the volume is increased, the probability of failure will increase as well. As originally derived, the Weibull formalism was established for isotropic materials under uniaxial tension, and the determination of the dependence of the probability of failure on the sample size can thus be evaluated.

For instances where materials are not under uniaxial tension, the statistical method of Weibull can be adapted [2–9] by considering the spatial distribution of stress in a body when loaded. Such an approach has been used for the well-defined geometries used to test the strength of brittle materials, namely, for 3-point bend specimens, for torsional bending of circular rods, and for ball-on-plate geometries. This approach is fruitful because these well-

defined geometries are subjected to the application of a constant load and also because the material properties of the body are not changing spatially and temporally.

While the methodology of Weibull statistics, in principle, can be applied to the case of binder burnout, a number of complications arise. The stresses occurring in binder burnout do not arise as a constant, externally applied, known load, but rather arise as an internal stress which varies with time and position in the body as the temperature in the furnace is increased. The material properties are also not isotropic and, furthermore, are changing locally with time as the binder, which gives strength to the body, is removed. While a number of studies [10–26] have addressed, from a modeling viewpoint, the stresses which arise during binder burnout, verification of the predicted pressure distributions and hence stress distributions has not been reported.

In a recent study, Liau *et al*. [26] fabricated barium titanate capacitors of square parallelepiped shape with poly(vinyl butyral) (PVB) binder and Pt electrodes in a range of different sizes. These MLCs were then subjected to different heating schedules. After binder burnout, the types of defects observed were cracks, fracture, and delamination—all defects of a brittle-like failure mode. The dependence of MLC yield on the dimensions of the samples was then established. As an outcome of this analysis, the existence of an optimum geometry for maximum yield was demonstrated with a height to length ratio of approximately 1 : 3. It was also observed that the gas-phase decomposition products flowed preferentially in the direction parallel to the metal electrode layers, suggesting different permeabilities in the directions parallel and perpendicular to the metal layers.

As the need arises for increased charge storage capacity, and thus larger multilayer devices, knowledge of the optimum capacitor geometry for maximum yield during binder burnout becomes increasingly important. In this work, results are presented for the optimum aspect ratio of capacitors of square parallelepiped geometry and for the penalty in yield associated with deviations from the optimum geometry. The approach developed is then extended to different geometries, and a methodology is presented for determining the optimum geometry given experimental data for the dependence of yield on sample dimensions.

2. Experimental

Capacitors were fabricated from 300 μm thick tapes consisting of barium titanate powder (Tamtron X7R412H, Tam Ceramics Inc., Niagara Falls, NY) with poly(vinyl butyral) as a binder (B73305, Ferro Corporation, San Marcos, CA). The capacitors were of square parallelepiped geometry (see Fig. 1) with side lengths between $L = 1.3$–3.8 cm and heights between $h = 0.3$–1.3 cm. The volume of these MLCs thus spanned roughly 1.5 orders of magnitude, from 0.5 to 19 cm^3, and the corresponding aspect ratios spanned 1 order of magnitude from $h/L = 0.08$ to 1. The platinum metal electrodes (E1192, Ferro Corporation, San Marcos, CA) were screen-printed at a thickness of nominally 5–10 μm. The tapes were then laminated at 2–4 MPa (300–600 psi) at 80–85 °C.

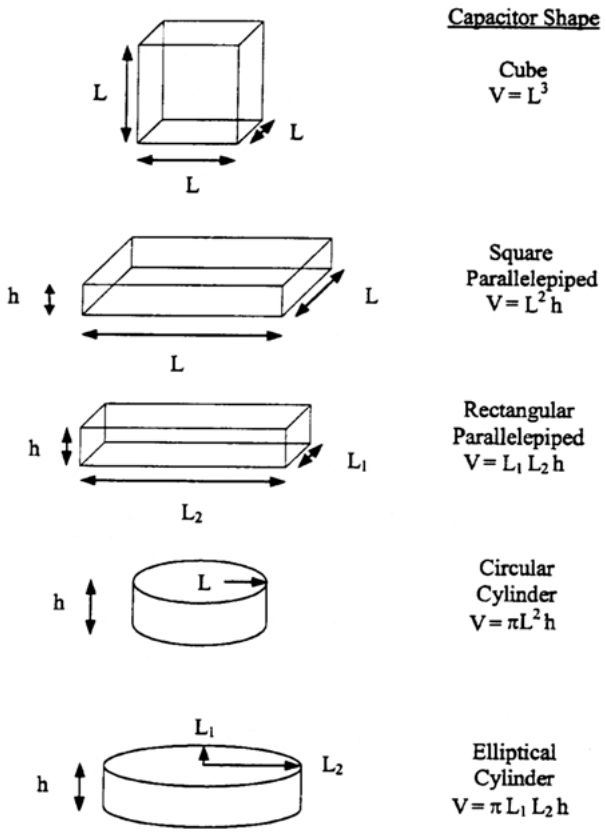

Figure 1 Schematic of capacitor shapes indicating the relevant dimensions, and volumes.

The heating schedules used for the binder burnout cycles were determined by first measuring the weight loss of binder in air as a function of temperature with a thermogravimetric analyzer. The weight loss data were then analyzed by a first-order kinetic model to determine the activation energy and pre-exponential factor. The degradation kinetics were next incorporated into a coupled heat and mass transfer model for describing the evolution of internal pressure within the samples as a function of time, temperature, and position. This procedure is described in more detail elsewhere [26].

Based on the results of the kinetic and modeling analysis, it was determined that fast heating rates could be used as long as holds were placed at the proper points in the burnout cycle. Three burnout cycles were evaluated using ramp rates of 1 °C min^{-1} in an air-atmosphere box furnace. The first cycle, which contained no low-temperature hold, consisted of a linear heating ramp to 600 °C, a 1-h hold at this temperature, followed by a 1 °C min^{-1} cooling rate to room temperature. The second cycle used contained a 10-h hold at 95 °C whereas the third cycle evaluated had a 10-h hold at 95 °C and a 10-h hold at 105 °C. After firing, the MLC samples were visually inspected for defects in order to determine the yield.

3. Results

The yield of MLCs of square parallelepiped geometry of different heights and lengths is displayed in Fig. 2. For samples fired according to the heating schedule with no low-temperature holds, the samples of smallest side length and smallest height survive at yields of 100%. For

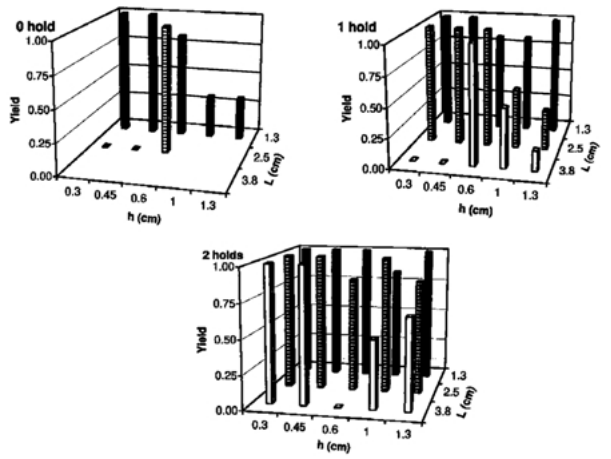

Figure 2 Yield of $BaTiO_3$-PVB-Pt multi-layer capacitors as a function of the dimensions of the capacitors and the number of holds in the heating cycle. From Liau *et al.* [26].

a constant side length of 1.3 cm, increasing the height leads to a decrease in yield. As the side length is increased from 1.3 to 2.5 cm, the samples of smallest height had zero yield whereas samples at $h = 0.6$ cm and $L = 2.5$ cm (an h/L ratio of 0.24) survived with no failures.

A second set of MLCs was fired according to a heating schedule containing one 10-h hold at 95 °C. Although the yield is improved as compared to the results contained in Fig. 2 for the cycle having no holds, samples corresponding to the larger values of side length and height generally survive at lower yield as compared to samples fabricated at smaller dimensions.

A third set of MLCs was fired according to a cycle containing two 10-h holds at 95 °C and 105 °C. For this 2-holds cycle, the yield is generally improved compared to what was observed in Fig. 2 for cycles containing no holds and one hold, even though the total cycle time is still less than 50 h.

An alternative way to view the response of yield to the number of holds in the cycle is to average all the yield data for a given cycle. As seen in Fig. 3a, a greater than two-fold improvement in the yield is observed as the number of holds is increased from zero to two. To evaluate the dependence of yield on side length, the data in Fig. 2 were averaged over the different thicknesses for each cycle, and as seen in Fig. 3b, the yield losses are substantial at the larger values of L.

To determine the explicit dependence of the yield, Y, on the side dimensions, $L_1 = L_2 = L$, and on the height, h, the data in Fig. 2 were analyzed by regression analysis according the function

$$Y = H - 2mL - nh \tag{1}$$

where H is a constant for a given furnace cycle. The coefficients determined in this manner were $m = 0.095$ and $n = 0.27$. The larger value of the coefficient n indicates a more detrimental dependence on the height as compared to the side length.

The different dependences of yield on the dimensions L and h indicate that for a given capacitor volume, a specific geometry of capacitor exists for maximum yield. To establish this optimum, the equation of volume for a square parallelepiped, $V = L^2h$, can be used to eliminate

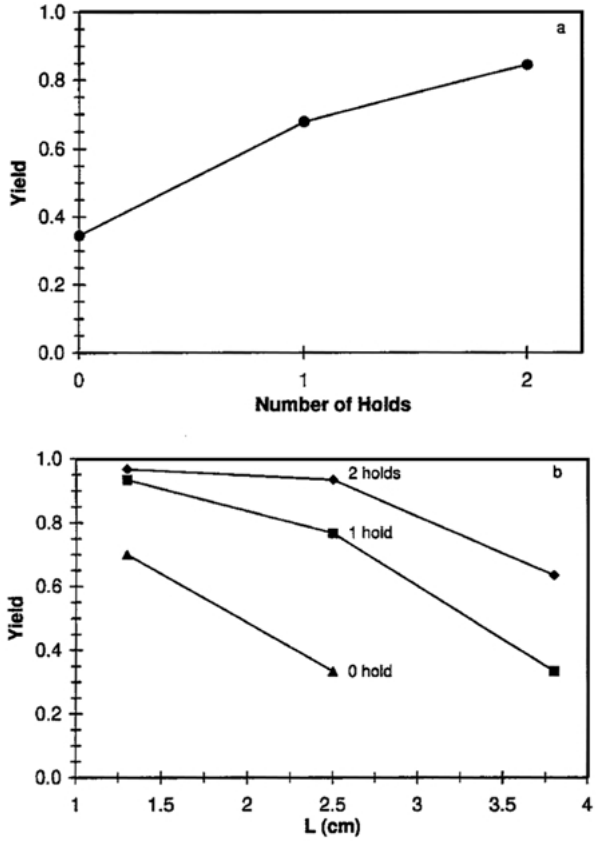

Figure 3 Yield of $BaTiO_3$-PVB-Pt multi-capacitors as a function of (a) the number of holds in the heating cycle and (b) the side length of the capacitors.

h from Equation 1. The resulting equation can then be differentiated at constant volume

$$\left(\frac{\partial Y}{\partial L}\right)_V = 0 = -2m + \frac{2nV}{L^3} \tag{2}$$

to determine the optimum height, h_o, optimum side length, L_o, and optimum aspect ratio, h_o/L_o:

$$L_o = \left(\frac{nV}{m}\right)^{1/3} \tag{3a}$$

$$h_o = \left(\frac{m^2V}{n^2}\right)^{1/3} \tag{3b}$$

$$\frac{h_o}{L_o} = \frac{m}{n} \tag{3c}$$

Equations 3a–b can also be obtained by augmenting Equation 1 by the constraint of volume and then applying the method of Lagrange multipliers. Equation 3c indicates that for the capacitors considered here, the optimum aspect ratio is $h_o/L_o = 0.35$ or a roughly 1 : 3 aspect ratio, and is independent of volume.

The second derivative of Equation 1 at constant volume is

$$\left(\frac{\partial^2 Y}{\partial L^2}\right)_V = -\frac{6nV}{L^4} \tag{4}$$

Since Equation 4 is always negative for a capacitor of finite dimensions, the optimum yield corresponds to a maximum. Fig. 4 demonstrates the yield as a function of

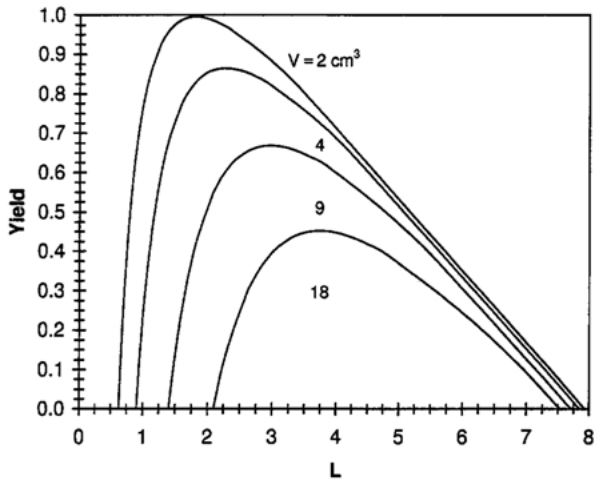

Figure 4 Yield as a function of side length and volume for square parallelepiped capacitors.

L for capacitors of different volumes. It is apparent that a maximum yield exists for every volume and that the yield decreases as the volume of the capacitors increases. Although the data in Fig. 4 indicate that the optimum varies with L, Fig. 5 demonstrates that the optimum h/L ratio is independent of volume and occurs at $h/L = 0.35$, in accordance with Equation 3c.

When, because of design considerations it is not possible to fabricate components at precisely the optimum aspect ratio, the topology of the yield surface determines the penalty in yield for designing at other aspect ratios. The fractional reduction in yield at constant volume, $\Delta Y(h,L)_V$, associated with not operating at the optimum values of h_o and L_o is given by

$$\Delta Y(h,L)_V = -2m\Delta L - n\Delta h \tag{5}$$

The deviations from the optimum side length, ΔL, and optimum height, Δh, are related to the constant volume restriction: $h_o L_o^2 = (h_o + \Delta h)(L_o + \Delta L)^2$. The reduction in yield is thus given by

$$\Delta Y(h,L)_V = \frac{\Delta L}{L_o}\left[\frac{nh_o(2 + \Delta L/L_o)}{(1 + \Delta L/L_o)^2} - 2mL_o\right] \tag{6}$$

Fig. 6 demonstrates that the penalty associated with moving away from the optimum depends asymmetrically on the fractional change in side length and also depends upon the volume of the capacitor, with larger capcitors exhibiting a larger penalty for not operating at the optimum aspect ratio.

While in the work of Liau *et al*. [26] a linear dependence of yield on h and L to the first power was treated for capacitors of square parallelepiped geometry, it is quite conceivable that other dependences on the dimensions may arise as well. These other cases are examined next, and the results are then extended to other capacitor geometries of rectangular, circular and elliptical shape, which are depicted in Fig. 1.

For the case of a capacitor of square parallelepiped geometry where the yield depends on the same coefficients and on the dimensions raised to the same positive exponent, α, the yield can be represented as

$$Y = H - 2mL^{\alpha} - mh^{\alpha} \tag{7}$$

By using the same mathematical techniques described previously, the optimum yield can be found at $h = L$, $(h_o/L_o = 1)$ which corresponds to a cube. Equation 7 can also represent the case of a capacitor of circular cylinder geometry of radius, L, height, h, and volume, $V = \pi L^2 h$; the optimum geometry for maximum yield occurs at $h = L$. Thus, an equal dependence on all dimensions leads to highly symmetrical capacitor shapes for maximum yield.

When the coefficients preceding the dimensions are unequal but the dependence on the dimensions is to the same positive exponent, α, the yield is given as

$$Y = H - 2mL^{\alpha} - nh^{\alpha} \tag{8}$$

and the optimum aspect ratio for maximum yield is

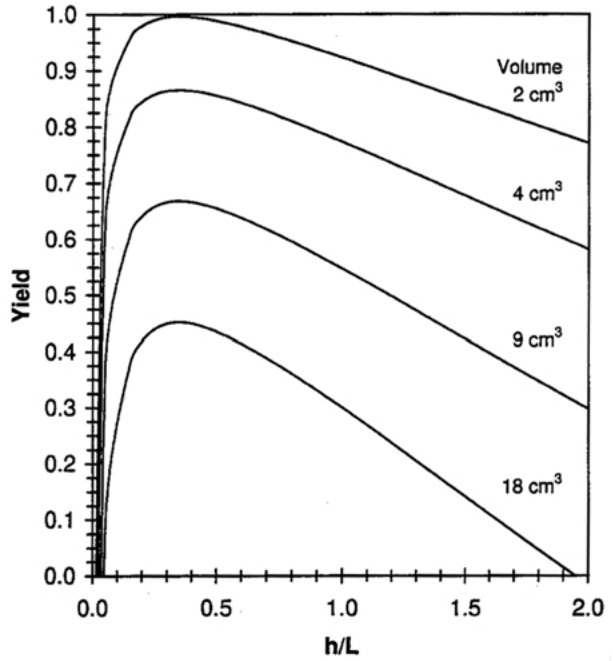

Figure 5 Yield as a function of aspect ratio and volume for square parallelepiped capacitors. The maximum yield is independent of the aspect ratio.

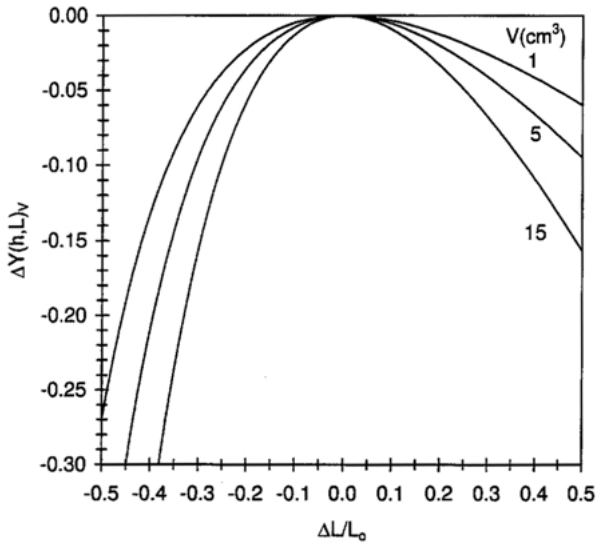

Figure 6 Fractional reduction in yield associated with not operating at the optimum aspect ratio for square parallelepiped capacitors of different volumes.

$$\frac{h_0}{L_0} = \left(\frac{m}{n}\right)^{1/\alpha} \tag{9}$$

which is seen to be independent of volume. For $\alpha = 1$, we recover Equation 3c. For capacitors of circular cylinder geometry of radius, L, and height, h, the optimum geometry can also described by Equation 9. Thus, different dependences of the yield on the dimensions leads to less symmetrical shapes for maximum yield as compared to the preceding case given by Equation 7.

The last case to be evaluated for a square parallelepiped geometry is for unequal coefficients preceding the dimensions with two unequal positive exponents, α and β. For this more general case, the yield is given by

$$Y = H - 2mL^{\alpha} - nh^{\beta} \tag{10}$$

and the optimum aspect ratio for maximum yield is

$$\frac{h_0}{L_0} = \left(\frac{m\alpha}{n\beta}\right)^{\frac{3}{(2\beta+\alpha)}} V^{\frac{(\alpha-\beta)}{(2\beta+\alpha)}} \tag{11}$$

which is now seen to depend on volume. For a capacitor of circular cylinder geometry of radius, L, and height, h, Equation 11 is valid with V replaced by V/π. Fig. 7 displays the dependence of the optimum aspect ratio on capacitor volume for different values of the exponents α and β. For $\alpha = \beta$, the optimum aspect ratio is independent of the volume and increases as the exponents increase. For $\alpha = 1$ and $\beta = 2$, the optimum aspect ratio decreases with increasing volume whereas for $\alpha = 2$ and $\beta = 1$, the optimum aspect ratio increases with increasing volume.

The trends observed in Fig. 7 indicate that for a fixed geometry, the optimum aspect ratio is sensitive to the values of the exponents α and β for fixed values of m and n. When acquiring data from experiments, data sets of greater than 5 samples per condition may be required to accurately determine m and n as a consequence of the statistical nature of defect populations. The influence of assuming the incorrect dependence of the yield on the exponents was thus assessed in the following manner. The values of $m = 0.095$ and $n = 0.27$ obtained in the experiments were used to generate yield results from Equation 10 for $\alpha = \beta = 1$. The data were then re-analyzed for two cases, assuming $\alpha = \beta = 0.5$ and $\alpha = \beta = 2$. The coefficients determined from this approach and the optimum aspect ratio are summarized in Table I. Although the coefficients are seen to depend on the values of the exponents assumed in the analysis, the optimum aspect ratio varies less than 10% from 0.33–0.38 for the data used here.

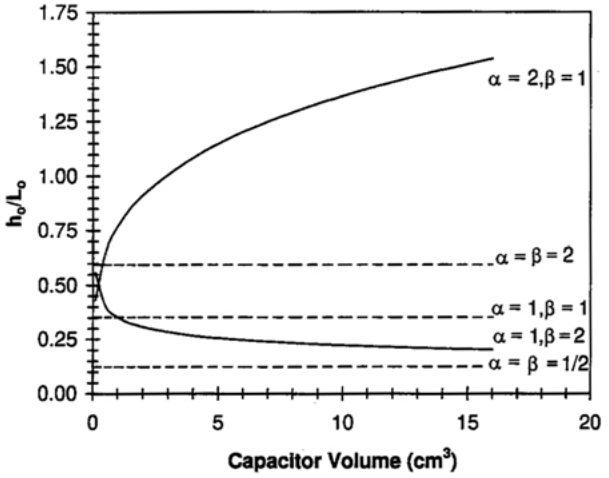

Figure 7 Optimum aspect ratio for square parallelepiped capacitors as a function of volume and the exponents α and β.

The yield analysis represented by Equations 1–10 corresponds to three-dimensional bodies with sufficient symmetry to be uniquely described by two length scales. The final geometries to be evaluated correspond to capacitors of lower symmetry where three length scales are required, as indicated in Fig. 1 for capacitors of rectangular parallelepiped geometry and elliptical cylinder geometry. To distinguish unambiguously between the length scales, L_1 is taken as smaller than L_2.

The first case to be addressed is for equal coefficients preceding the dimensions and for any positive α-order exponent on the dimensions. For the general case of a rectangular parallelepiped of dimensions L_1, L_2 and h, the yield is given by

$$Y = H - mL_1^{\alpha} - mL_2^{\alpha} - mh^{\alpha} \tag{12}$$

The optimum geometry for a maximum in yield is attained when $L_1 = L_2 = h$, independent of volume, and thus a cubed-shaped capacitor is the optimum design under these circumstances. The same type of analysis holds for an elliptical cylinder capacitor of principal radii, L_1 and L_2, and height, h. The optimum geometry for maximum yield is a circular cylinder capacitor with $L_1 = L_2 = h$.

For the geometry of a square parallelepiped treated by Equations 1, 7, 8, and 10, the geometry was prescribed. We now show how this geometry arises from the treatment of a rectangular parallelepiped of side lengths, L_1 and L_2 and height, h, with equal coefficients preceding L_1 and L_2. For any positive α-order dependence on dimensions, the yield is given by

$$Y = H - mL_1^{\alpha} - mL_2^{\alpha} - nh^{\alpha} \tag{13}$$

For this case, it can be shown that at the optimum, $L_1 = L_2$ and the optimum geometry is a square parallelepiped. The optimum ratio of h/L is given by

$$\frac{h_0}{L_0} = \left(\frac{m}{n}\right)^{1/\alpha} \tag{14}$$

The same analysis leading to Equation 14 can also be applied to a capacitor whose planes are elliptical of radii, L_1 and L_2 and of height, h. For this case, the optimum geometry is obtained when $L_1 = L_2$, which corresponds to a capacitor of circular cylindrical shape. Thus, equal dependences of yield on two length scales leads to shapes of high symmetry in the plane containing them.

When the complexity of the dependence is further increased such that all the coefficients are unequal but the positive exponent α is the same, the yield is given by

$$Y = H - m_1L_1^{\alpha} - m_2L_2^{\alpha} - nh^{\alpha} \tag{15}$$

The optimum values of the dimensions are then

$$L_{1,0} = V^{1/3}\left(\frac{m_2 n}{m_1^2}\right)^{1/3\alpha} \tag{16a}$$

TABLE I Dependence of the optimum aspect ratio on the exponents used in the model

	$\alpha = \beta = 0.5$	$\alpha = \beta = 1$	$\alpha = \beta 2$
m	0.52	0.095	0.01
n	0.91	0.27	0.07
h_o/h_o	0.33	0.35	0.38

$$L_{2,0} = V^{1/3}\left(\frac{m_1 n}{m_2^2}\right)^{1/3\alpha} \tag{16b}$$

$$h_0 = V^{1/3}\left(\frac{m_1 m_2}{n^2}\right)^{1/3\alpha} \tag{16c}$$

and are now seen to depend on volume. For $m_1 \neq m_2$, the dimensions L_1 and L_2 would be different, and thus the optimum geometry would correspond to a capacitor of rectangular parallelepiped shape.

For the final case of $L_1 \neq L_2$ with unequal coefficients and unequal positive exponents, the yield is described as

$$Y = H - m_1 L_1^{\alpha} - m_2 L_2^{\beta} - nh^{\gamma} \tag{17}$$

For this case, the optimum values of the dimensions are given by

$$L_{1,0} = \left[V\left(\frac{m_2\beta}{m_1\alpha}\right)^{1/\beta}\left(\frac{n\gamma}{m_1\alpha}\right)^{1/\gamma}\right]^{\frac{1}{\alpha(1/\alpha+1/\beta+1/\gamma)}} \tag{18a}$$

$$L_{2,0} = \left[V\left(\frac{m_1\alpha}{m_2\beta}\right)^{1/\alpha}\left(\frac{n\gamma}{m_2\beta}\right)^{1/\gamma}\right]^{\frac{1}{\beta(1/\alpha+1/\beta+1/\gamma)}} \tag{18b}$$

$$h_0 = \left[V\left(\frac{m_1\alpha}{n\gamma}\right)^{1/\alpha}\left(\frac{m_2\beta}{n\gamma}\right)^{1/\beta}\right]^{\frac{1}{\gamma(1/\alpha+1/\beta+1/\gamma)}} \tag{18c}$$

and are more complex than the expressions developed previously for cases of higher symmetry.

4. Discussion

The degradation of polymer and flow of decomposition products during binder burnout represents a coupled heat transfer, mass transfer, and reaction kinetics problem. The generation of unequal pressures of gas-phase decomposition products within the body, which leads to internal stresses within the ceramic green body, is a problem in continuum mechanics. Since the concentration of binder is changing spatially and temporally during the heating cycle, and thus the material properties are also changing, the overall coupling between the reaction, transport, and stress effects becomes quite complex. As demonstrated by the yield results presented here, full solution of the yield problem also necessarily requires a multi-dimensional modeling approach.

Multi-layer ceramic capacitors are composite structures with planes of ceramic and binder being separated by metal electrode layers. In the work of Liau *et al*. [26], the gas-phase decomposition products were observed to flow preferentially out of the body in the direction parallel to the metal layers. This observation suggests that the permeability of the green body is different in the directions parallel and perpendicular to the metal layers. Consequently, the pressure distribution and the resulting stress distribution are expected to have strong directionality in the body as well.

The unequal dependence of yield on the dimensions of the body thus gives rise to an optimum capacitor shape. This optimum design presumably minimizes the pressure fields and hence stress fields in the body. The real situation is slightly more complex, however, in that brittle fracture occurs when the stress fields coincide with flaws of sufficient size to lead to failure. More precisely, then, the optimum capacitor geometry minimizes the failure probability of a stress coupling with a flaw within the body.

The methodology presented in this work allows for yield data acquired from binder burnout experiments to be used to determine the optimum dimensions of capacitors. From these optimum dimensions, the pressure and hence stress distributions may be inferred, but this remains to be firmly established. Since asymmetry in the pressure distribution arises as a consequence of different permeabilities in different directions within the capacitor, the yield expressions developed in this work may ultimately have a link to the directionality of permeability within the green body.

5. Conclusions

The yield of capacitors of square parallelepiped geometry has been shown to exhibit unequal dependences on the length and height of the body, and thus an optimum height-to-length ratio exists for maximum yield. When not operating at the optimum aspect ratio, a reduction in yield occurs. Expressions have been developed to quantify this loss, which is seen to depend on the volume of the capacitor.

The approach used to obtain the optimum geometry from the analysis of experimental data has been generalized to develop expressions for the design of capacitors of rectangular, circular cylinder, and elliptical cylinder shapes. These results can then be used to guide the design of capacitor shapes so that improved yield during binder burnout can be realized.

References

1. J. A. LEWIS, *Annu. Rev. Mater. Sci.* **27** (1997) 147.
2. W. WEIBULL, *Ing. Vetenskaps. Akad. Handl.* **151** (1939) 1.
3. W. WEIBULL, *ibid.* **153** (1939) 1.
4. B. EPSTEIN, *J. Appl. Phys.* **19** (1948) 140.
5. B. EPSTEIN, *Am. Stat. Assoc. J.* **43** (1948) 403.
6. ''Probabilistic Methods in the Mechanics of Solids and Structures'', edited by S. Eggwertz and N. C. Lind (Springer-Verlag, Berlin, 1984).
7. H. L. OH and I. FINNIE, *Int. J. Fract. Mech.* **6** (1970) 287.
8. F. A. MCCLINTOCK, in ''Fracture Mechanics Of Ceramics'', vol. 1, edited by R. C. Bradt, D. P. H. Hasselman and F. F. Lange (Plenum Press, NY, 1973) pp. 93–114.
9. Y. MATSUO and K. KITAKAMI, in ''Fracture Mechanics of Ceramics'', vol. 7, edited by R. C. Bradt, A. G. Evans, D. P. H.

Hasselman and F. F. Lange (Plenum Press, NY, 1986) pp. 223–253.
10. M. R. BARONE and J. C. ULICNY, *J. Am. Ceram. Soc.* **73** (1990) 3323.
11. J. A. LEWIS and M. J. CIMA, *ibid.* **73** (1990) 2702.
12. P. CALVERT and M. CIMA, *ibid.* **73** (1990) 575.
13. M. J. CIMA, J. A. LEWIS and A. D. DEVOE, *ibid.* **72** (1989) 1192.
14. J. R. G. EVANS, M. J. EDIRISINGHE, J. K. WRIGHT and J. CRANK, *R. Soc. London A* **432** (1991) 321.
15. S. A. MATAR, M. J. EDIRISINGHE, J. R. G. EVANS and E. H. TWIZELL, *J. Mater. Res.* **8** (1993) 617.
16. S. A. MATAR, M. J. EDIRISINGHE, J. R. G. EVANS, E. H. TWIZELL and J. H. SONG, *J. Mater. Sci.* **30** (1995) 3805.
17. J. H. SONG, M. J. EDIRISINGHE, J. R. G. EVANS and E. H. TWIZELL, *J. Mater. Res.* **11** (1996) 830.
18. S. A. MATAR, M. J. EDIRISINGHE, J. R. G. EVANS and E. H. TWIZELL, *J. Am. Ceram. Soc.* **79** (1996) 749.
19. R. M. GERMAN, *Int. J. Powder Metall.* **23** (1987) 237.
20. B. K. LOGRASSO and R. M. GERMAN, *Powder Metall. Int.* **22** (1990) 17.
21. G. Y. STANGLE and I. A. AKSAY, *Chem. Eng. Sci.* **45** (1990) 1719.
22. D.-S. TSAI, *AIChE J.* **37** (1991) 547.
23. A. MANGUIN-FRITSCH, H. BURLET, P. M. FOURT and M. ABOUAF, *L'Industrie Céram. Verrière* **887** (1992) 744.
24. A. C. WEST and S. J. LOMBARDO, *Chem. Eng. J.* **71** (1998) 243.
25. T. S. SHIVASHANKAR and R. M. GERMAN, *J. Am. Ceram. Soc.* **82** (1990) 1146.
26. L. C.-K. LIAU, B. PETERS, D. S. KRUEGER, A. GORDON, D. S. VISWANATH and S. J. LOMBARDO, *J. Am. Ceram. Soc.* **83** (2000) 2645.

Received 17 July 2000
and accepted 15 February 2001